Global Warming and Marine Carbon Cycle Feedbacks on Future Atmospheric CO_2

Fortunat Joos,* Gian-Kasper Plattner, Thomas F. Stocker, Olivier Marchal, Andreas Schmittner

A low-order physical-biogeochemical climate model was used to project atmospheric carbon dioxide and global warming for scenarios developed by the Intergovernmental Panel on Climate Change. The North Atlantic thermohaline circulation weakens in all global warming simulations and collapses at high levels of carbon dioxide. Projected changes in the marine carbon cycle have a modest impact on atmospheric carbon dioxide. Compared with the control, atmospheric carbon dioxide increased by 4 percent at year 2100 and 20 percent at year 2500. The reduction in ocean carbon uptake can be mainly explained by sea surface warming. The projected changes of the marine biological cycle compensate the reduction in downward mixing of anthropogenic carbon, except when the North Atlantic thermohaline circulation collapses.

Carbon dioxide is the most important anthropogenic greenhouse gas that contributes to anthropogenic climate change. Projections of future atmospheric CO_2 levels, based on carbon emissions scenarios (*1*), are affected by considerable uncertainties because of a limited understanding of the mechanisms driving carbon sequestration by the ocean and the land biota.

We investigated a potentially important positive feedback loop that involves atmospheric CO_2, global warming, the hydrological cycle, ocean circulation, and the marine carbon cycle in a world of continued carbon emissions. Rising atmospheric CO_2 leads to increased radiative forcing (*2*), resulting in higher sea-surface temperatures (SSTs) and a stronger hydrological cycle that may reduce sea surface salinity at high latitudes (*3, 4*). These changes may induce a reorganization of the thermohaline circulation (THC) and a collapse of the North Atlantic Deep Water (NADW) formation (*3, 5*), a reorganization of the marine carbon cycle (*6–8*), and a reduction in the surface-to-deep transport of anthropogenic carbon. The resulting reduction in oceanic carbon uptake may in turn accelerate the atmospheric CO_2 growth.

Carbon dioxide ice core measurements (*9, 10*) suggest a small sensitivity of atmospheric CO_2 to rapid and large changes in the marine carbon cycle for the last glacial period. However, an extrapolation of the glacial situation to the future is not straightforward.

Recent modeling studies (*6–8, 11*) have investigated only parts of the feedback loop described above. Maier-Reimer *et al*. (*6*) prescribed the global warming pattern in their prognostic ocean biogeochemical model. They concluded that the weakening of the ocean circulation, in combination with the more effective biological utilization of surface nutrients, has a small influence on future atmospheric CO_2 levels. On the other hand, Sarmiento and colleagues (*7, 11*) applied a diagnostic marine biological model with fixed biological export fluxes and prescribed atmospheric CO_2 growth in their coupled atmosphere-ocean model. They suggested that a THC weakening and a SST increase reduce ocean carbon uptake by up to 50% and that such reductions are only partly offset by changes in the marine biological cycle (*12*).

We have used a low-order physical-biogeochemical climate model that consists of a zonally averaged ocean model (*13*), coupled to an atmospheric energy balance model (*14*) and a representation of the marine (*15*) and terrestrial (*16*) carbon cycle (*17*). Radiative forcing has been calculated in all simulations from atmospheric CO_2 assuming a logarithmic dependence (*18, 19*). The climate sensitivity of the energy balance model (that is, the increase in global mean surface air temperature for a doubling of atmospheric CO_2, $\Delta T_{2\times}$) was set to 3.7°C, identical to that of the Geophysical Fluid Dynamics Laboratory's coupled three-dimensional (3D) atmosphere-ocean model (*3*). This temperature is at the higher end of the range of 1.5° to 4.5°C, which was estimated by others (*2*). We also carried out "baseline" simulations, where radiative forcing was kept constant by setting $\Delta T_{2\times}$ to 0°C (constant climate and ocean circulation).

Results were compared with the box-diffusion–type "Bern" carbon cycle model (*20, 21*) used in past assessments (*2, 22*) of the Intergovernmental Panel on Climate Change (IPCC) and with an updated version that includes an energy balance model to forecast sea surface warming and its effect on the CO_2 partial pressure (pCO_2) (*23*). Unlike in the 2D model, ocean transport was kept constant in the Bern model.

We present three sets of simulations. First, atmospheric CO_2 (Fig. 1C) was calculated from prescribed carbon emissions until year 2100 from the IPCC IS92a, IS92c, and IS92e emissions scenarios (*1*) (Fig. 1A). The modeled NADW formation decreased by 30 to 60% until year 2100, indicating substantial changes in ocean circulation (Fig. 1B). The differences in the increase of atmospheric CO_2 between the baseline ($\Delta T_{2\times}$ = 0°C) and the standard ($\Delta T_{2\times}$ = 3.7°C) 2D simulations

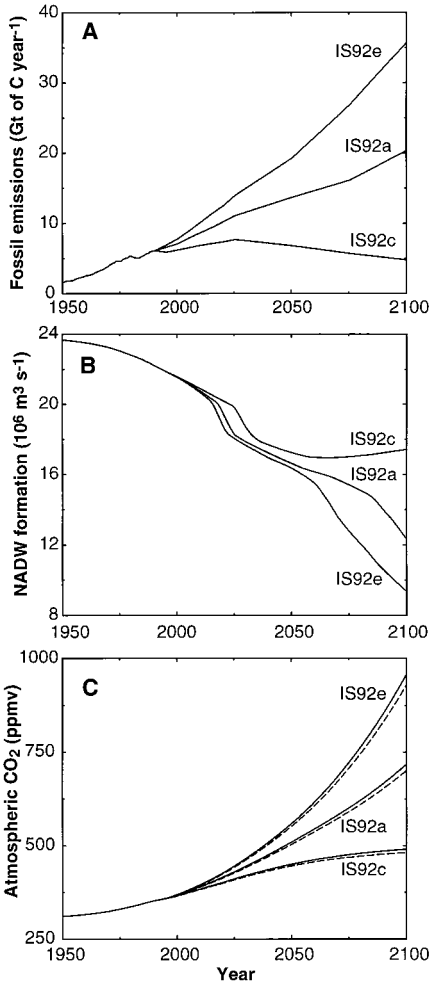

Fig. 1. (**A**) Carbon emissions in 10^{12} kg of carbon per year (Gt of C $year^{-1}$) for the IPCC IS92a, IS92c, and IS92e scenarios (*1*). The scenarios depict potential evolutions of carbon emissions based on estimates of future population growth and economic development. (**B**) NADW formation when atmospheric CO_2 and radiative forcing were calculated from emissions shown in (A) and $\Delta T_{2\times}$ = 3.7°C. (**C**) Projected atmospheric CO_2 for the emissions shown in (A) for the baseline ($\Delta T_{2\times}$ = 0°C) (dashed lines) and the standard ($\Delta T_{2\times}$ = 3.7°C) (solid lines) simulations.

Climate and Environmental Physics, Physics Institute, University of Bern, Bern, Switzerland.

*To whom correspondence should be addressed. E-mail: joos@climate.unibe.ch

are ~4% for the period from years 1765 to 2100. This small difference is explained by the emission pathway that allowed the ocean to absorb only a relatively small part of the emissions (one-third for IS92a) and by the modest change in ocean uptake.

Second, atmospheric CO_2 was prescribed with the IPCC CO_2 profiles (Fig. 2A), resulting in the stabilization of atmospheric CO_2 at levels between 350 and 1000 parts per million by volume (ppmv) [WRE350 to WRE1000 (*22, 24*)]. The profiles were used to investigate implications for future carbon emissions. NADW formation decreases substantially for all profiles and even collapses for WRE1000 (Fig. 2B). Global carbon emissions (Fig. 2C) were calculated as the sum of the prescribed atmospheric carbon inventory change and the modeled oceanic and terrestrial uptake. For the WRE550 profile, 28% of the cumulative emissions until year 2500 remained airborne, whereas 51 and 21% were sequestered by the ocean and the terrestrial biosphere, respectively. Differences in cumulative emissions between the simulations of $\Delta T_{2\times} = 3.7°C$ and $\Delta T_{2\times} = 0°C$ are between 3% (WRE1000) and 6% (WRE350) for the period from years 1765 to 2100 and ~9% (for all WRE profiles) for the period from years 1765 to 2500 (Fig. 2C). Results obtained with the Bern model are in close agreement with our 2D model results (Fig. 2C), except when NADW formation stops (Fig. 2B, WRE1000 profile).

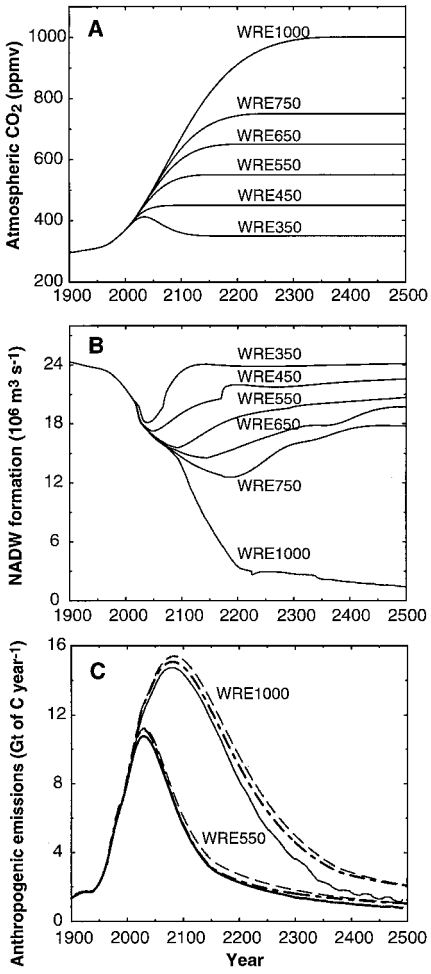

Fig. 2. (**A**) Profiles resulting in the stabilization of atmospheric CO_2 at levels between 350 and 1000 ppmv (WRE350, WRE450, WRE550, WRE650, WRE750, and WRE1000) considered by IPCC (*2*). The profiles follow the observed concentration history until the present and then approximately follow the IS92a concentration path for the next decades to eventually approach a stabilization level. (**B**) NADW formation for the CO_2 profiles shown in (A) and $\Delta T_{2\times} = 3.7°C$. (**C**) Global anthropogenic carbon emissions that are consistent with the WRE1000 and WRE550 CO_2 profiles shown in (A) for the baseline ($\Delta T_{2\times} = 0°C$) (dashed lines) and the standard ($\Delta T_{2\times} = 3.7°C$) (solid lines) simulations. Anthropogenic emissions as obtained by the Bern model (dashed-dotted lines) are given for comparison (*2, 22*).

Third, emissions were prescribed until year 2500 to study the full feedback loop over longer time scales. Emissions were taken from the baseline ($\Delta T_{2\times} = 0°C$) WRE550 and WRE1000 simulations (Fig. 2C). Projected atmospheric CO_2 at year 2500 is then, by definition, 550 and 1000 ppmv for $\Delta T_{2\times} = 0°C$. For $\Delta T_{2\times} = 3.7°C$, projected CO_2 at year 2500 is 593 and 1156 ppmv. Thus, the atmospheric CO_2 increase at year 2500 would be underestimated by 16% (WRE550) and 22% (WRE1000) when adopting an emission pathway to CO_2 stabilization with the baseline model. Correspondingly, the global mean surface air temperature increase until year 2500 would be underestimated by 0.4°C for WRE550 and by 0.6°C for WRE1000. That is ~10% of the realized warming.

We conclude from the three simulation sets that atmospheric CO_2 exhibits a small sensitivity to global warming until year 2100 and that global emissions consistent with a CO_2 stabilization pathway are similar for simulations with and without global warming. These findings are in line with paleoreconstructions that show little CO_2 variations during past abrupt (decadal-scale) climatic changes (*9, 10*). In any case, carbon emissions need to be reduced below the present level to achieve a stabilization of atmospheric CO_2 (*2, 22*).

Differences in cumulative ocean uptake between simulations with $\Delta T_{2\times} = 0°C$ and $\Delta T_{2\times} = 3.7°C$ are ~10% (years 1765 to 2100) for the profiles stabilizing CO_2 at or below 750 ppmv (WRE350 to WRE750).

Table 1. Ocean uptake for different model setups and the WRE550 CO_2 profile. In simulation A (baseline, no feedbacks), the climate sensitivity, $\Delta T_{2\times}$, was set to 0°C. In simulation B (standard, all feedbacks), SST, freshwater fluxes, ocean circulation, and biological cycling were described by prognostic formulations, and $\Delta T_{2\times}$ is 3.7°C. In simulation C (SST feedback), SSTs that were used to determine the surface-water pCO_2 were from simulation B; all other parameters were as in the baseline simulation A. In simulation D (SST + circulation feedback), the physical model was used as in simulation B, and the marine biota feedback was excluded. Organic matter export was diagnosed at each time step so that surface-water PO_4 concentrations remained at preindustrial values. Surface-water alkalinities were prescribed with the distribution at the end of the spin-up. In simulation E (SST + circulation + biota-DIC feedback), salinity normalized surface-water alkalinities were kept at their preindustrial values, whereas other parameters were set as in the standard simulation B. In simulation F (constant export), export fluxes of organic material and $CaCO_3$ were kept at their preindustrial values except when surface-water PO_4 concentrations approach zero; then organic matter export was set to zero.

Simulation	Parameters	Years		
		1980 to 1989	1765 to 2100	1765 to 2500
	Model experiments: Cumulative ocean uptake (Gt of C)			
A	Baseline (no feedback, $\Delta T_{2\times} = 0°C$)	21.4	530	1240
B	Standard (all feedbacks, $\Delta T_{2\times} = 3.7°C$)	20.2	480	1030
C	SST	18.9	462	1024
D	SST + circulation	18.6	447	996
E	SST + circulation + biota-DIC	20.5	494	1121
F	Constant export fluxes	21.0	498	1067
	Estimated reduction in ocean uptake by main feedbacks (%)			
A − C	SST	11.7	12.7	17.4
C − D	Circulation	1.4	2.9	2.3
D − B	Biota	−7.5	−6.1	−2.7
A − B	Total reduction	5.6	9.5	17.0
	Estimated reduction in ocean uptake by differentiation of biota feedbacks (%)			
D − E	Biota-DIC	−8.9	−8.8	−10.0
E − B	Biota-alkalinity	1.4	2.7	7.3
	Reduction in ocean uptake for different implementations of the marine biota (%)			
A − F	Constant export production	1.9	6.0	14.0
A − B	Standard prognostic version	5.6	9.5	17.0
A − D	No biota feedback	13.1	15.6	19.7
(A − B) − (D − E)	No biota-DIC feedback	14.5	18.3	27.0

This is similar to the reduction range of 4 to 14% found by comparable studies (*6*–*8*). The difference reaches 27% at year 2500 for a stabilization at 1000 ppmv (WRE1000) where NADW formation stops (Fig. 2B). This is again comparable to the 28% reduction in CO_2 uptake found by Sarmiento and Le Quéré (*7*) when stabilizing CO_2 at 1200 ppmv. Apparently, the differences between the various models do not result in very different estimates of the overall reduction.

The importance of different oceanic processes for the reduction in CO_2 uptake was estimated by running the model in different setups (*25*) (simulations A through F, Table 1 and Fig. 3). We found that both a reduction in the CO_2 solubility caused by increasing SST ("SST feedback," simulation A − C) and the reduction in surface-to-deep transport of anthropogenic carbon ("circulation feedback," simulation C − D) decrease oceanic uptake, whereas changes in the cycling of marine organic material and $CaCO_3$ ["marine biota feedback," simulation D − B (*26*)] partly compensate the reduction. The SST feedback is by far the most dominant feedback with respect to CO_2 uptake in our model, except when NADW formation stops (Fig. 3). Therefore, modifications of the CO_2 solubility by increasing sea surface temperatures should be considered in projections of future atmospheric CO_2.

The marine biota feedback is dictated in the model by the slower circulation in the standard ($\Delta T_{2\times}$ = 3.7°C) than in the baseline ($\Delta T_{2\times}$ = 0°C) simulation. This results in lower export fluxes and lower inputs of nutrients and alkalinity into the euphotic zone. The net effect is a reduction in surface-water PO_4 and alkalinity. A reduction in surface-water PO_4 is associated with a reduction in surface-water dissolved inorganic carbon (DIC) concentrations ("biota-DIC feedback"), which is partly compensated by increased oceanic carbon uptake, whereas a reduction in alkalinity ("biota-alkalinity feedback") decreases uptake. In our model, the biota-DIC feedback dominates the biota-alkalinity feedback (Table 1).

To explore the sensitivity of the marine biosphere model, we constructed a hypothetical "no biota-DIC feedback" case to obtain upper limit estimates for the CO_2 uptake reduction. Only the biota-alkalinity feedback and the circulation and SST feedbacks were considered; the reduction by the biota-DIC feedback (Table 1, simulation D − E) was subtracted from the reduction by all feedbacks (Table 1, simulation A − B). This corresponds to a situation in which the marine ecosystem composition shifts toward a high abundance of $CaCO_3$ producers (*27*), whereas organic matter export is reduced by the same amount as nutrient supply into the surface waters. For the WRE550 profile, the reduction in ocean uptake is 27% until year 2500 (Table 1).

Next, we performed a simulation in which the export fluxes of organic material and $CaCO_3$ were kept at their preindustrial values (Table 1, simulation F). This assumption yields lower estimates for the CO_2 uptake reduction. Surface-water PO_4 (and DIC) concentrations are reduced when the surface-to-deep mixing is reduced. For the WRE550 profile, the reduction in ocean uptake is 24% until year 2500. More extreme scenarios, in which surface-water nutrient concentrations

Table 2. Sensitivity of ocean carbon uptake to variations in the climate sensitivity, $\Delta T_{2\times}$, and the vertical eddy diffusivity, K_v, for the WRE550 CO_2 profile. Uptake values for $\Delta T_{2\times}$ = 0°C are shown in parentheses for K_v values. Standard values are 0.4 × 10^{-4} m^2 s^{-1} for K_v and 3.7°C for $\Delta T_{2\times}$.

Parameter value	Cumulative ocean uptake in Gt of C		Reduction from 1765 to 2500
	1980 to 1989	1765 to 2500	
	Variation of $\Delta T_{2\times}$ (°C)		
0.0	21.4	1240	0.0%
1.5	20.8	1154	6.9%
2.5	20.2	1087	12.3%
3.7	20.2	1030	17.0%
4.5	19.4	981	20.9%
	Variation of K_v (10^{-4} m^2 s^{-1})		
0.6	22.9	1128 (1349)	16.5%
0.4	20.2	1030 (1240)	17.0%
0.2	18.2	934 (1116)	16.3%

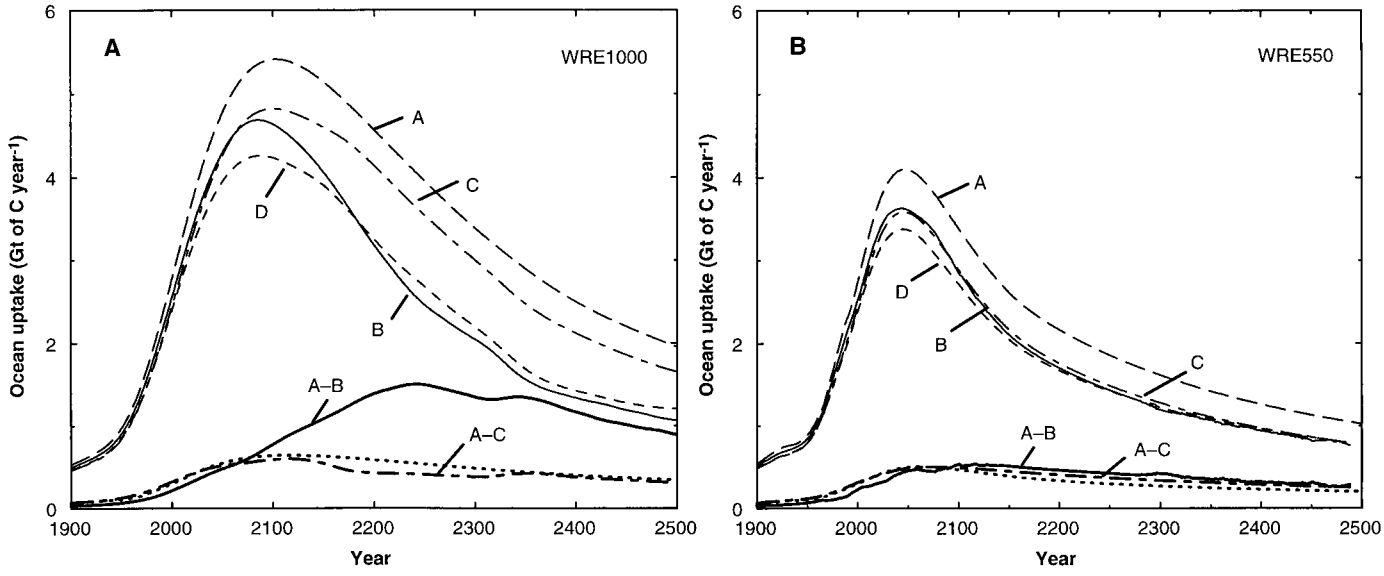

Fig. 3. Ocean carbon uptake and reduction in carbon uptake for simulations in which selected feedbacks are operating (see Table 1 and main text) for the (**A**) WRE1000 and the (**B**) WRE550 CO_2 stabilization profiles. The reduction in CO_2 uptake by all feedbacks is the difference between simulation A and B (A − B) (thick solid line). The SST feedback is the difference between simulation A and C (A − C) (thick dotted-dashed line). The SST feedback simulated by the Bern model is shown by the thick dotted line. The circulation feedback is the difference between simulation C (dotted-dashed line) and D (short-dashed line). The biota feedback is the difference between simulation D (short-dashed line) and B (solid line).

were completely exhausted, have been previously published in the context of proposals for large-scale fertilization of the marine biosphere (*28*).

The different formulations of the marine carbon cycle produce ranges for the reduction in CO_2 uptake under the WRE550 profile of 6 to 18% and of 14 to 27% for the periods of years 1765 to 2100 and 1765 to 2500, respectively (Table 1). Our results suggest that only extreme changes in marine ecosystem structure, such as those assumed in the no biota-DIC feedback scenario, result in a substantially different ocean uptake than in our standard simulation.

We also performed tests where the climate sensitivity $\Delta T_{2\times}$ was varied between 1.5° and 4.5°C while atmospheric CO_2 was prescribed according to the most extreme IPCC profile (WRE1000). Modeled circulation shows a bifurcation at $\Delta T_{2\times} = 3.0$°C, beyond which the NADW formation completely collapses (Fig. 4). The collapse is delayed by ~115 years for $\Delta T_{2\times} = 3.05$°C in comparison to our standard climate sensitivity of $\Delta T_{2\times} = 3.7$°C. The effect of a complete versus a partial breakdown in NADW formation was investigated by comparing CO_2 uptake for $\Delta T_{2\times}$ above ($\Delta T_{2\times} = 3.05$°C) and below ($\Delta T_{2\times} = 3.00$°C) the bifurcation point. For the period from years 2200 to 2500, ocean uptake is reduced from 900 Gt of carbon (baseline, $\Delta T_{2\times} = 0$°C) to 700 Gt of carbon ($\Delta T_{2\times} = 3.00$°C) and to 590 Gt of carbon ($\Delta T_{2\times} = 3.05$°C). The additional reduction in uptake of 110 Gt of carbon indicates that a potential near-term collapse of the North Atlantic THC would have a profound impact on atmospheric CO_2.

The sensitivity of oceanic carbon uptake and simulated atmospheric CO_2 to changes in the climate sensitivity, $\Delta T_{2\times}$, is similar to changes in the vertical eddy diffusivity of the model (Table 2). We varied the model's constant vertical eddy diffusivity coefficient between 0.2×10^{-4} and 0.6×10^{-4} m^2 s^{-1}. Then, the average oceanic uptake during the 1980s varies between 1.8 and 2.3 Gt of carbon per year, which is well within the current range of 2.0 ± 0.8 Gt of carbon per year (*2, 29*), and the cumulative uptake for the period from years 1765 to 2500 varies between 930 and 1130 Gt of carbon for WRE550. This is comparable to the range of 981 to 1240 Gt of carbon when $\Delta T_{2\times}$ is varied between 4.5° and 0°C, and this indicates that the uncertainties in carbon uptake associated with changes in SST, circulation, and marine biosphere are of a similar magnitude as uncertainties that are associated with our incomplete knowledge of the rates of surface-to-deep transport.

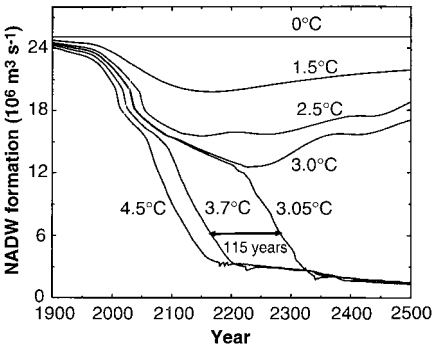

Fig. 4. Dependence of the NADW formation on the climate sensitivity, $\Delta T_{2\times}$, varied between 0° and 4.5°C (*2*) for the WRE1000 CO_2 profile (Fig. 2A). The collapse in NADW formation is irreversible for $\Delta T_{2\times}$ values that are higher than 3°C.

The feedbacks could potentially be detected by atmospheric observations (*11*). Measurements of O_2/N_2 can be used to determine the oceanic carbon uptake (*30*). We projected the evolution of the atmospheric carbon isotope ratio $\delta^{13}C$ that is influenced by the SST, the circulation, and the biota feedback and the change in the carbon isotope ratio $\Delta^{14}C$ that is influenced by the circulation feedback only. For WRE1000, the difference between baseline and standard simulations is 14% (0.23 per mil) for $\delta^{13}C$ and 3% (6 per mil) for $\Delta^{14}C$ of the predicted isotopic changes between years 2000 and 2100. This is of the same order as uncertainties in the prediction of atmospheric $\delta^{13}C$ and $\Delta^{14}C$, indicating that the feedbacks are difficult to detect by atmospheric carbon isotope measurements alone. We suggest that sustained ocean surveys aimed at detecting potential circulation changes and carbon cycle feedbacks should be performed.

References and Notes

1. J. Legget, W. J. Pepper, R. J. Swart, *Climate Change 1992: The Supplementary Report to the IPCC Scientific Assessment* (Cambridge Univ. Press, New York, 1992), pp. 69–95.
2. J. T. Houghton *et al*., *Climate Change 1995—The Science of Climate Change: Contribution of WGI to the Second Assessment Report of the Intergovernmental Panel on Climate Change* (Cambridge Univ. Press, New York, 1996).
3. S. Manabe and R. J. Stouffer, *J. Clim.* **7**, 5 (1994).
4. U. Mikolajewicz and R. Voss, *Technical Report 263* (Max-Planck-Institut für Meteorologie, Hamburg, Germany, 1998), pp. 1–27.
5. T. F. Stocker and A. Schmittner, *Nature* **388**, 862 (1997).
6. E. Maier-Reimer, U. Mikolajewicz, A. Winguth, *Clim. Dyn.* **12**, 711 (1996).
7. J. L. Sarmiento and C. Le Quéré, *Science* **274**, 1346 (1996).
8. R. J. Matear and A. C. Hirst, *Tellus Ser. B*, in press.
9. B. Stauffer *et al*., *Nature* **392**, 59 (1998).
10. O. Marchal *et al*., *Clim. Dyn*., in press.
11. J. L. Sarmiento, T. M. C. Hughes, R. J. Stouffer, S. Manabe, *Nature* **393**, 245 (1998).
12. In the model applied by Sarmiento and colleagues (*7, 11*), the most important changes occur in the Southern Ocean. A different mixing scheme results in a smaller change in the Southern Ocean (*8*).
13. D. G. Wright and T. F. Stocker, *J. Geophys. Res.* **97**, 12707 (1992).
14. T. F. Stocker, D. G. Wright, L. A. Mysak, *J. Clim.* **5**, 773 (1992).
15. O. Marchal, T. Stocker, F. Joos, *Tellus Ser. B* **50**, 290 (1998).
16. U. Siegenthaler and H. Oeschger, *ibid.* **39**, 140 (1987).
17. Parameters and boundary conditions of the model are as in (*5, 15*). The marine biological model is based on the classical Redfield approach, and PO_4 is used as a limiting nutrient for biological production. For the land biosphere, a potential fertilization by elevated atmospheric CO_2 is taken into account by a logarithmic dependence of net primary production on CO_2 (*21*).
18. K. Shine, R. G. Derwent, D. J. Wuebbles, J.-J. Morcrette, in *Climate Change: The IPCC Scientific Assessment*, J. T. Houghton, G. J. Jenkins, J. J. Ephraums, Eds. (Cambridge Univ. Press, Cambridge, 1990), pp. 41–68.
19. We neglected the radiative forcing by other greenhouse gases, thereby assuming that the additional forcing by anthropogenic methane, nitrous oxide, halocarbons, and ozone was roughly offset by the cooling induced by anthropogenic sulfate aerosols. In the IPCC IS92 scenarios and in the reference stabilization profiles discussed in (*22*), radiative forcing resulting from CO_2 only differs by ~10% from the forcing by all gases and aerosols, except for the two lowest stabilization profiles. The deviations are small in comparison to the overall range of forcings considered.
20. U. Siegenthaler and F. Joos, *Tellus Ser. B* **44**, 186 (1992).
21. F. Joos *et al*., *ibid.* **48**, 397 (1996).
22. D. Schimel *et al*., in *IPCC Technical Paper III, Stabilisation of Atmospheric Greenhouse Gases: Physical, Biological, and Socio-economic Implications*, J. T. Houghton, L. G. Meira Filho, D. J. Griggs, K. Maskell, Eds. (Intergovernmental Panel on Climate Change, Geneva, 1997), pp. 1–48.
23. F. Joos and M. Bruno, *Phys. Chem. Earth* **21**, 471 (1996).
24. T. M. L. Wigley, R. Richels, J. A. Edmonds, *Nature* **379**, 240 (1996).
25. The attribution of the carbon uptake reduction to different mechanisms is only an approximation because the ocean-atmosphere carbon cycle system is nonlinear. The validity of our attribution was checked by running additional simulations and an inorganic model.
26. In our terminology, the marine biota feedback with respect to oceanic carbon uptake is zero if surface-water PO_4, the limiting nutrient, and alkalinity remain unchanged. In the standard simulation, carbon uptake is enhanced by the marine biota feedback, although export production is reduced. The quantity that is relevant for atmospheric CO_2 is not the strength of the export production but how the biological cycle affects the surface distribution of alkalinity and DIC through changes in the balance between supply to and biological export out of the surface layer. The biota feedback is driven in the model mainly by circulation changes that modify the nonlinear interplay between the production at surface and the remineralization at depth of particulate and dissolved organic matter and $CaCO_3$, the transport of nutrients and alkalinity into the surface ocean, the carbonate chemistry, and the CO_2 air-sea fluxes.
27. It is not clear whether calcification will increase or decrease in the future. Calcification might increase with increasing SST or decrease because CO_3^{2-} concentrations decrease with increasing pCO_2.
28. F. Joos, J. L. Sarmiento, U. Siegenthaler, *Nature* **349**, 772 (1991).
29. U. Siegenthaler and J. L. Sarmiento, *ibid.* **365**, 119 (1993).
30. R. F. Keeling, S. C. Piper, M. Heimann, *ibid.* **381**, 218 (1996).

31. We thank E. Maier-Reimer for helpful comments. This work was supported by the European Commission Programme Climate and Environment (grants ENV4-CT97-0495, ENV4-CT95-0130, ENV4-CT95-0131, and ENV4-CT97-0643), the Swiss Federal Office for Science and Education (grants 97.0414, 95.0470, 95.0471, and 97.0414), and the Swiss National Science Foundation.

2 December 1998; accepted 9 March 1999